



Flow characteristics and energy dissipation over stepped spillway with various step geometries: case study (steps with curve end sill)

Udai A. Jahad¹ · Ali Chabuk¹ · Riyadh Al-Ameri² · Hasan Sh. Majdi³ · Ali Majdi³ · Nadhir Al-Ansari⁴ · Salwan Ali Abed⁵

Received: 6 June 2022 / Accepted: 23 January 2024 / Published online: 29 February 2024
© The Author(s) 2024

Abstract

Stepped weirs are used in a wide range of applications, designed to increase energy dissipation. In this study, laboratory experiments were conducted in a flume on six stepped weir models, with a downstream angle of $\theta = 26.6^\circ$. The physical models used were on a scale of 10:1, and tests of discharges up to $0.055 \text{ m}^3/\text{s}$ were carried out. Several step geometries including traditional step, sill and curve geometries were used to study flow behavior and overall energy dissipation. The laboratory investigations were augmented by modelling numerically the within step flow and energy behavior using a 2-D CFD model, incorporating the k- ϵ model for turbulence closure. The results showed that energy dissipation was greatest for the curved steps by about 10.5%, where it was observed that the skimming flow regime was shifted to a higher discharge range. Numerical modelling results showed good agreement with the experimental results. An inspection of the modelled streamlines highlighted the increase in vortex intensity for the curve model, reflecting the strong circulation observed. The predicted stepwise energy dissipation showed the energy dissipation increase when the step number N_s increases. For the range of step height h_s , tested, our results showed that energy dissipation increased with step height. The results from this study can be used to inform engineering design for steps with $\theta = 26.6^\circ$ and provide estimates of the expected energy dissipation and residual energy.

Keywords Energy dissipation · Stepped · Modified step · Spillway · Flow regime

Introduction

Stepped spillways are hydraulic structures with energy dissipating properties. According to Chanson (2015), a stepped spillway can be characterized as an energy dissipator and air

entrainment. Also, the step configuration is the main factor in generating flow resistance resulting in energy dissipation. It is leading to a decrease in flow velocity. Dhattrak and Tatewar (2014) investigated the flow regimes in case nappe and skimming regimes. In nappe flow, “the flow from each step

✉ Nadhir Al-Ansari
alansari@ltu.se

Udai A. Jahad
eng.udai.jahad@uobabylon.edu.iq

Ali Chabuk
ali.chabuk@uobabylon.edu.iq

Riyadh Al-Ameri
r.alameri@deakin.edu.au

Hasan Sh. Majdi
dr.hasanshaker@mustaqbal-college.edu.iq

Ali Majdi
alimajdi@mustaqbal-college.edu.iq

Salwan Ali Abed
salwan_ali2000@yahoo.com

¹ Department of Environment Engineering, College of Engineering, University of Babylon, Babylon 51001, Iraq

² School of Engineering, Deakin University, 75 Pigdons Road, Waurin Ponds, VIC 3220, Australia

³ Al-Mustaqbal University College, Babylon 51001, Iraq

⁴ Department of Civil Environmental and Natural Resources Engineering, Lulea University of Technology, SE-971 87, Lulea, Sweden

⁵ College of Science, Al-Qadisiyah University, Al Diwaniyah, Iraq

hits the step below as a falling jet, with the energy dissipation occurring by a jet breakup in air, jet mixing on the step, with or without the formation of a partial hydraulic jump on the step”, and in skimming flow, “the water flows down the stepped face as a coherent stream, skimming over the steps and cushioned by the recirculating fluid trapped between them”. Early observations of energy dissipation suggest that dissipation rates “appears to be enhanced by the momentum transfer to the recirculating fluid”. Three different kinds of flow regimes can be seen in the flow over the stepped spillway depending on the affecting factors. Nappe flow for low discharges, skimming flow for high discharges, and transition flow (Wan et al., 2019; Kaouachi et al. 2021).

Roushangar et al. (2014) have found that the dissipation of energy in stepped spillways is significant and the stepped spillway is an effective means of dissipating excess flow energy. Felder and Chanson (2015) showed that an increase in step height increases energy dissipation for the same number of steps. Zhou et al. (2020) conducted an experimental study to evaluate the stepped spillway performance and compared the results with a smooth spillway. The energy dissipation was better in nappe flow than in the skimming flow regime. Felder (2013) studied the energy dissipation between stepped spillways with uniform and non-uniform step heights and reported that energy dissipation rates were similar. Torabi et al. (2018) investigated energy dissipation on stepped spillways with flat steps with different roughness. Two types of roughness elements, uniform roughness consisting of sand with given grain size, and discrete roughness consisting of fine blocks of specific dimensions were investigated. The results showed that for the nappe flow regime, the energy dissipation increased by about 15–20% for steps with roughness elements compared with smooth steps.

Other laboratory studies have also been undertaken to modify the step geometry in order to improve energy dissipation. Jahad et al. (2016) studied the effectiveness of adding curved end sills at step edges. Their results show that curved end sills-edged chutes have higher energy dissipation than the sill edge, resulting in about 5% more energy dissipation compared to a flat step-stepped spillway. Wu et al. (2016) investigated aeration and energy dissipation in stepped spillways employing an entrance section, ski-jump, pre-step section, aeration basin, and a stepped chute. The authors reported that their model improved energy dissipation and cavitation damage was reduced by about 8%, compared to a traditional stepped spillway. Mero et al. (2017) studied the use of differently shaped steps of moderate slope (26.6°) and showed that the energy dissipation rate was about two times more than flat steps.

There have also been numerical modelling studies on stepped spillways (e.g., Peng 2015; Lopez-Egea et al. 2015; Daneshfaraz et al. 2020; Kaouachi et al. 2021; Lebdiri et al. 2020, 2022). According to Castillo et al. (2014), different turbulence closure models have been implemented with the Reynolds-Averaged Navier–Stokes equations have been used. Dong et al (2019) utilized multiphase flow Computational Fluid Dynamics (CFD) models, to assist several dams in China with stepped spillways. The equation of Reynolds-averaged Navier–Stokes has been solved. The simulated flow pattern and recirculation region agreed well with experimental results, although the CFD model provided more accurate simulations of the velocity profile. Hamed and Ketabdar (2016) used experimental and a finite volume method with the standard k- ϵ model numerical approach to study the flow characteristics and energy dissipation for stepped spillways with normal end sills. The results showed reasonable agreement between the experimental and numerical approaches for both flow regimes and energy dissipation. Lebdiri et al. (2020) investigated the impacts of the step number on energy dissipation rate, the acted shear stresses on the walls for the flow stepped spillway. Ansys-Fluent is used in modelling to solve Navier–Stokes equations with both VOF and turbulent k- ϵ . The results encouraged the researchers to use the CFD approach. CFD model can show the inside hydraulic variations which cannot be shown physically sometimes.

The above review shows that stepped spillways have received considerable attention due largely to their importance in civil engineering. Most of the early work focused on energy dissipation, largely investigated by physically modelling. In this respect, modifications of the step geometry are a promising feature in increasing energy dissipation, given the success reported in the literature. However, further shapes and geometries need to be tested. More importantly, the area of study that is still lacking is numerical prediction; although some studies have been conducted, modelling of stepped spillways with steps of different geometries is either limited or non-existent. The motivation for this study was therefore to improve our understanding of stepped spillways’ performance, particularly the hydraulics behind and energy dissipation characteristics of these structures, as a function of step shape and geometry. Using a laboratory and numerical modelling approach to study step spillways with a variety of shapes and geometries, the objectives for this study therefore were: (i) assess the energy dissipation and flow characteristics of step spillways in a laboratory flume, (ii) numerically investigate flow and energy dissipation characteristics, and (iii) suggest optimal geometry for the step shapes and geometries studied.

Methodology

Laboratory experiments

Laboratory experiments were carried out in a 7.0 m long, 0.5 m wide, and 0.6 m deep flume. Discharge Q (L/s) was measured by a flowmeter with an accuracy of ± 1 L/s. The flow was supplied from a storage 3.0m^3 via a 0.2 m diameter pipe to the inlet tank and straightened before entrance into the flume before exiting via a free overfall. Three different steps geometries, each with 2 different geometries, resulting in a total of 6 experimental setups, were tested. All six setups had a total length $L=0.7$ m and spillway height $H_d=0.3$ m, giving a chute angle $\theta=26.6^\circ$. The models were manufactured from plywood with a roughness height of $k_s \approx 0.4$ mm. The steps numbers are $N_s=6$ and 10 with step heights of $h_s=0.05$ m and 0.03 m, respectively as shown in Table 1 and Fig. 1. The three shapes comprised: (i) rectangular shape or Step Model (Fig. 1(a) and (b)), where Step_1 has ten flat steps with step height ($h_s=0.03$ m) and Step_2 has six flat steps with step height ($h_s=0.05$ m), (ii) rectangular shape with an end sill or Sill Model (Fig. 1(c) and (d)), where Sill_1 has ten steps (height of the end sill equals step height $h_s=0.03$ m) and Sill_2 has six steps (height of the end sill equals step height $h_s=0.05$ m), and (iii) quarter-circle curve step or Curve Model (Fig. 1(e) and (f)), where Curve_1 has ten steps (height of the quarter circle equals $h_s=0.03$ m) and Curve_2 has six steps (height of the quarter circle equals $h_s=0.05$ m). All the test setups were made from plywood and finished with a coat of marine paint to a smooth finish. The Step model was chosen as the basic shape, for comparison with previous studies conducted with the same chute angle, and ultimately with the Sill and Curve Models. The ranges of experimental parameters tested are provided in Table 1, where h_s and l_s are the step height and length, respectively, N_s is the number of the steps, and y_c is the critical flow depth. All tests were carried out twice, to test for repeatability. A total of 144 experimental runs were therefore conducted for unit discharges, q ranging from 9.0 L/s.m. to a maximum of 111 L/s.m. Water depths were measured by point gauges, with an accuracy of $\pm 0.2\%$.

Previous studies by Torabi et al. (2018), Mero and Mitchell (2017), Wu et al. (2016), Tabari and Tavakoli (2016), and Li et al. (2014) have quantified energy dissipation, by measuring the difference in specific energies, ΔE , upstream and downstream of the stepped spillway. This is a relatively straightforward task as the specific energy, E , can be estimated based on water depth measurements.

Numerical modelling

ANSYS Fluent v18.1 (ANSYS® Academic Research 2017) CFD package using the Volume of Fluid (VOF) model has been used to numerically model flow behaviour. The VOF method is a multi-phase numerical modelling procedure proposed by Hirt and Nichols in 1981 and is used in free-surface flow problems. In the VOF method, the momentum equation is solved for two phases of non-miscible fluids, and the fraction occupied by each fluid phase in a computational cell is tracked. The model solves the incompressible continuity and momentum equations for turbulent flow Torrano et al. (2015):

$$\frac{\partial \rho}{\partial t} + \frac{\partial \rho u_i}{\partial x_i} = 0 \tag{1}$$

$$\begin{aligned} \frac{\partial \rho u_i}{\partial x_i} + \frac{\partial}{\partial x_i} (\rho u_i u_j) = & \\ - \frac{\partial p}{\partial x_i} + \frac{\partial}{\partial x_j} \left\{ \mu \left(\frac{\partial u_i}{\partial x_j} + \frac{\partial u_j}{\partial x_i} - \frac{2}{3} \delta_{ij} \frac{\partial u_k}{\partial x_k} \right) \right\} & \\ + \frac{\partial}{\partial x_j} (-\rho u_i' u_j') & \end{aligned} \tag{2}$$

where ρ is the density of the fluid, μ is molecular viscosity, u_i is the velocity component, x_i is the coordinate component, t is the time, and p is the pressure. The deviatoric stress component in Eq. (2) can be expressed as:

$$-\rho u_i' u_j' = \mu_t \left(\frac{\partial u_i}{\partial x_j} + \frac{\partial u_j}{\partial x_i} \right) - \frac{2}{3} (\rho k) \delta_{ij} \tag{3}$$

Table 1 Experimental parameters tested

Model	h_s (m)	l_s (m)	End sill type	End sill height (m)	N_s	$y_c h_s$
Step_1	0.03	0.067	–	–	10	0.66–1.05
Sill_1	0.03	0.067	normal	0.03	10	0.66–1.05
Curve_1	0.03	0.067	quarter circle	0.03	10	0.66–1.05
Step_2	0.05	0.120	–	–	6	0.69–1.08
Sill_1	0.05	0.120	normal	0.05	6	0.69–1.08
Curve_1	0.05	0.120	quarter circle	0.05	6	0.69–1.08

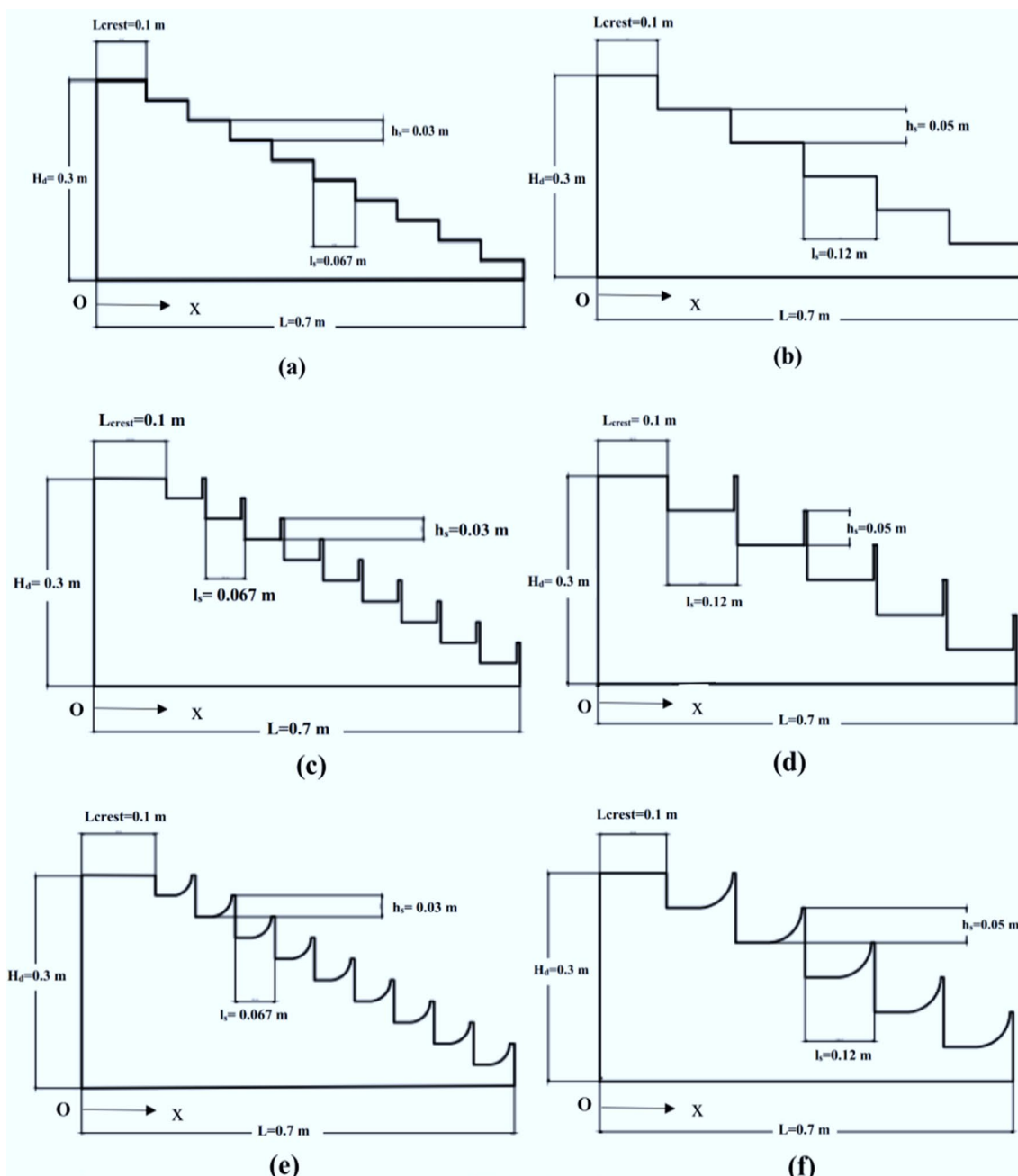


Fig. 1 Stepped spillways with different shape and dimensions tested. a Step_1, b Step_2, c Sill_1, d Sill_2, e Curve_1 and f Curve_2

where μ_t is the turbulent viscosity and the stress tensors $\delta_{ij} = 1$ when $i = j$ and $\delta_{ij} = 0$ when $i \neq j$, using the $k-\epsilon$ model for turbulence closure (Torrano et al. 2015):

$$\frac{\partial(\rho k)}{\partial t} + \text{div}(\rho k U) = \text{div} \left\{ \left(\frac{\mu_t}{\sigma_k} \right) \text{grad} k \right\} + 2\mu_t E_{ij} E_{ij} - \rho \epsilon \tag{4}$$

$$\frac{\partial(\rho \epsilon)}{\partial t} + \text{div}(\rho \epsilon U) = \text{div} \left\{ \left(\frac{\mu_t}{\sigma_\epsilon} \right) \text{grad} \epsilon \right\} + C_{1\epsilon} \frac{\epsilon}{k} 2\mu_t E_{ij} E_{ij} - C_{2\epsilon} \rho \frac{\epsilon^2}{k} \tag{5}$$

$$\mu_t = \rho C_\mu \frac{k^2}{\epsilon} \tag{6}$$

where, $C_u = 0.09$, $\sigma_k = 1.0$, $\sigma_\epsilon = 1.3$, $C_{1\epsilon} = 1.44$ and $C_{2\epsilon} = 1.92$ Torrano et al. (2015).

The numerical model was run, to steady-state, for all experimental conditions listed in Table 1. The boundary conditions do not change from one case to another except for the inlet velocity. The velocity inlet was calculated using continuity equations for five discharges ($Q = 4.35$ L/s,

10.10 L/s, 25 L/s, 38.46 L/s, and 55.55 L/s) from experimental work. The velocity was defined as velocity magnitude and the x-direction was used as a velocity direction in the ANSYS-Fluent software. The velocity was $v_o = 0.0275, 0.0605, 0.1326, 0.1895, \text{ and } 0.2566$ (m/s) as the data input in ANSYS-Fluent software for all the models, where v_o is the inlet velocity. The VOF model was used to simulate the two-phase flow (air and water) with the $k-\epsilon$ model to identify the turbulent flow turbulence in ANSYS-Fluent software. The numerical model was run to a steady state for all experimental conditions. The inlet boundary conditions were separated into two parts to account for air and water fluid components. The average velocity was set for the water flow component. The atmospheric pressure was specified for the air layer. The pressure outlet was taken as the outlet boundary condition for the water layer. In addition, atmospheric pressure was specified for the outlet air layer and top boundary. The flume bed and the surfaces of the steps were defined by the wall boundary (nonslip) condition.

Results and discussion

Laboratory experiments

Step model results and comparison with previous studies

Experiments with the Step_1 model show that nappe flow regime was maintained until $q = 8.6$ L/s.m, and $y_c/h_s = 0.66$. The onset of skimming flow occurred when $q \approx 20.0$ L/s.m or $y_c/h_s = 1.05$. In comparison, for the Step_2 model, the corresponding values for q are 20.0 L/s.m and 39.0 L/s.m, and y_c/h_s are 0.69 and 1.08, for nappe and skimming flow regimes respectively. Transition flow was observed in between these limiting values of q and y_c/h_s . Pictures of the three flow regimes for the Step Model are shown in Fig. 2, where Fig. 2a shows nappe flow for $q = 8.6$ L/s.m. Figure 2b shows the transition flow regime $q = 10.1$ L/s.m where it is observed that the flow is skimming in the upper steps and

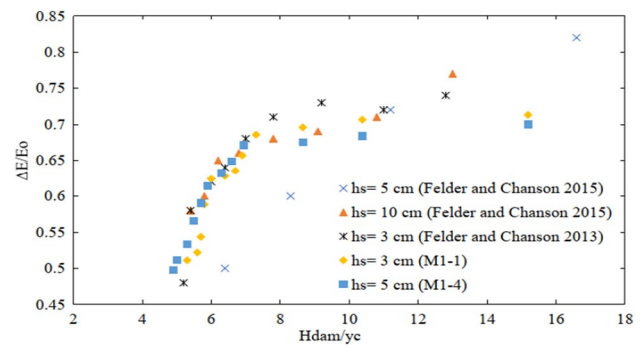


Fig. 3 Energy dissipation stepped spillways (flat step): comparison with previous studies

at lower steps, nappe. Skimming flow is present at higher discharge, $q = 39.0$ L/s.m (Fig. 2c).

Figure 3 compares ΔE for the Step Model as a function for H_d/y_c with previous studies for $\theta = 26.6^\circ$. In general, ΔE increases when discharge decreases or when H_d/y_c increases, consistent with studies by Felder and Chanson (2013) and Felder et al. (2015). The current study obtained higher energy dissipation for low discharges in all models. In models Step_1 and Step_2 at $q = 9.0$ L/m.s the $\Delta E/E_0 = 0.81$ and 0.75 respectively because of the nappe flow regime effects. Chanson (2015) defined the nappe flow regime as “the water proceeds in a series of plunges from one step to another and the flow from each step hits the step below as a falling jet”, which leads to an increase in flow resistance when compared with other flow regimes. Moreover, for high discharge (e.g. at $q = 111.0$ L/m.s) the energy dissipation was the lowest, $\Delta E/E_0 = 0.56$ and 0.55, respectively, because of skimming flow effects. Chanson (2015) characterized the skimming flow regime as water flowing downstream of the stepped spillway as a consequential stream, skimming on the steps and cushioned by the circulating water trapped between them. The differences between the two models can be attributed to the impact of the step height h_s and length l_s on the water surface profile and flow characteristics.

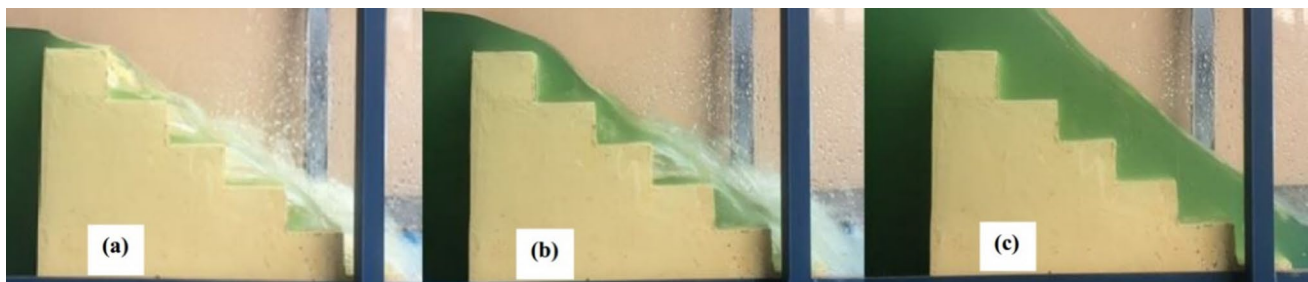


Fig. 2 Observed flow regimes for Step_2 model. **a** Nappe flow ($q = 8.6$ L/s.m, $y_c/h_s = 0.69$), **b** Transition flow (8.6 L/s.m $< q < 39.0$ L/s.m, $0.7 < y_c/h_s < 1.09$) and **c** Skimming flow ($q = 39.0$ L/s.m, $y_c/h_s = 1.08$)

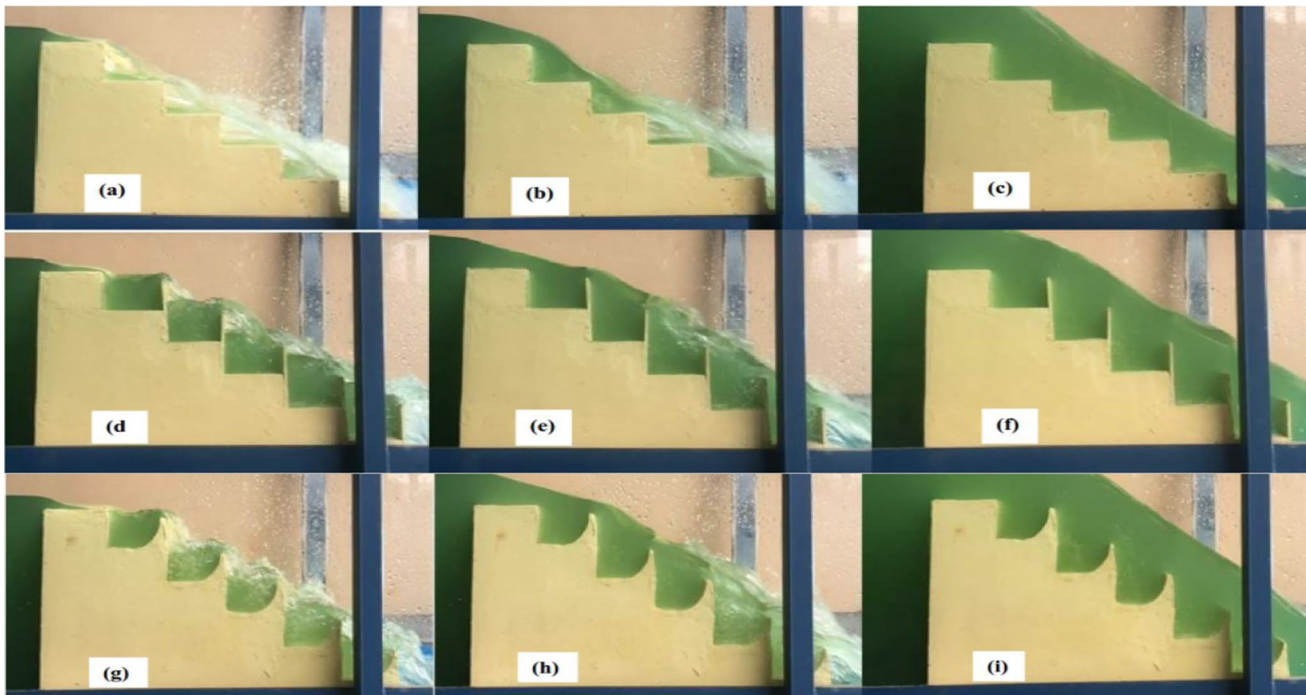


Fig. 4 Observed free surface for flow over stepped spillways. Nappe flow: **a** Step_2, **d** Sill_2 and **g** Curve_2, where $q=20.0$ L/s.m, $y_c/h_s=0.69$. Transition flow: **b** Step_2, **e** Sill_2 and **f** Curve_2, where

$20.0 < q < 39.0$ L/s.m, $0.07 \leq y_c/h_s \leq 1.09$. Skimming flow: **c** Step_2 **f** Sill_2 and **i** Curve_2, where $q=39.0$ L/s.m, $y_c/h_s=1.08$

Other step shapes and geometries

Figure 4 shows the typical flow regimes (Nappe, Transition, and Skimming) observed on the step geometries tested. In Sill_1 and Curve_1, the Nappe flow regime developed when $y_c/h_s = 1.16$, and in Sill_2 and Curve_2 models, at $=0.87$. At these values y_c/h_s , the flow regime was in Transition for Step_1 and Step_2 models. Skimming flow regime was observed at $y_c/h_s = 1.44$ for Sill_1 and Curve_1 and $y_c/h_s = 1.27$ for Sill_2 and Curve_2. Skimming flow appeared at lower y_c/h_s for Step_1 and Step_2 models ($y_c/h_s = 1.16$ and 1.08 , respectively). The observations that the Nappe and Transition flow regimes appear at higher values of y_c/h_s (or higher q) compared to the Step_1 and Step_2 models is attributed to the storage within the pools, particularly for the Curve models. In the Sill and Curve models (Fig. 4d to i), part of the flow is advected downstream, similar to the flat step, but a proportion of the flow is retained on the steps within the recirculation zones. The volume retained in the pools can be quite large, if q is small (Fig. 4d and g). The flow at a step is dominated by a hydraulic jump generated by the main flow, transiting from supercritical to subcritical flow within the step as the flow is decelerated by the sill. The main flow then accelerates as it plunges to the subsequent step, repeating the transition from supercritical to subcritical flow. These observations detail the effects of step height and

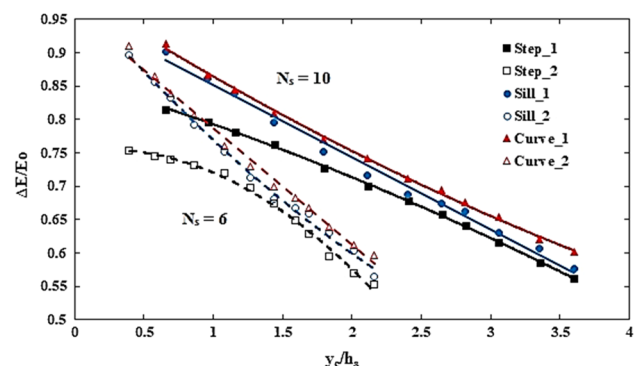


Fig. 5 Energy dissipation on stepped spillway with steps of various

end sills in influencing the hydraulic behaviour, enhancing energy dissipation rates.

Figure 5 compares ΔE for all the step geometries where it is observed that ΔE decreases with increasing y_c/h_s (increasing q). For nappe flow (low discharge), the energy loss is highest due to the interactions between the plunging flow with the individual steps. Energy loss however is observed to be higher for Curve and Sill compared to the Step model. The $\Delta E/E_0$ was higher for Curve_1 and Sill_1 model than the Step_1 model by 7% and 5%, respectively, with Curve_1 having the highest $\Delta E/E_0$. Similarly, $\Delta E/E_0$ was higher for model Curve_2 and Sill_2 than Step_2

by approximately 10% and 7%, respectively. The highest $\Delta E/E_0$ observed for Curve models is due to higher energy dissipation associated with the considerable influence of the semi-circular end sills. This influence might be due to the greater frictional resistance provided by the semi-circular shape which is more streamlined thus providing a greater contact area compared to the Sill or Step model. As flow approaches skimming, differences in $\Delta E/E_0$ became smaller for all models, since the effects of step geometry and geometry became less significant and the flow discharges down the stepped face as a coherent stream.

Numerical modelling

CFD model validation

The experimental approach was used to define the velocity downstream of the stepped spillway to obtain the CFD results. The solvers for stepped spillways were at the start of their assessment. Therefore, it is necessary to check the results. Furthermore, in this study, the CFD model was a parallel work to experiments. The root means square error (RMSE) and the mean absolute percentage error (MAPE) in (Eqs. 7 and 8) respectively are the criteria used to validate the CFD models.

$$RMSE = \sqrt{\frac{1}{n} \sum_1^n (V1_{\text{experimental}} - V1_{\text{CFD}})^2} \tag{7}$$

$$MAPE = 100 \times \frac{1}{n} \sum_1^n \left| \frac{V1_{\text{experimental}} - V1_{\text{CFD}}}{V1_{\text{experimental}}} \right| \tag{8}$$

Also, the correlation coefficient (R) was used as a tool to determine the quality of fit between the experimental and CFD results. Equation 9 was given to computed R.

$$R = \frac{C_{xyj}}{\sigma_x \sigma_y} \tag{9}$$

where: xi and yj are defined as the CFD and experimental output results, respectively; C_{xyj} is the covariance between the CFD (x_j) and the physical model results (y_j); σ_x and σ_y are the standard deviations of the CFD and the physical model results, respectively.

Table 2 presents a comparison between the experimental and CFD results. The statistical values such as R, MAPE, and RMSE were computed for verification. The benefit of MAPE and RMSE were used as an indicator for the error which should be zero or close to it. In the present study, the model has the index value nearest to zero which is considered more precise. As shown in Table 2, the MAPE and RMSE are 4.32, and 0.21 respectively with $R = 0.996$ for five values of the discharges. The RMSE was close to zero, it was signifying the best agreement.

Flow regime

The results from the CFD model run predicting flow regimes under different flow conditions are shown in Fig. 6(a) – (i) and compared with the experimental observations (Fig. 4(a) - (i), respectively) for the same flow conditions. In general, the predicted longitudinal water surface profiles are similar to the experimental results, and the flow characteristics observed in the model are consistent with the experimental observations. Nappe flow occurred in the experiments for $q \approx 20.0$ L/s.m and is reproduced by the numerical model (Fig. 6(a), (d), and (g)). The modelled free surface is noticed to be wavy and disturbed due to the plunging flow. In the experiments, it was observed that plunging flow, especially for the upper steps, in the Step model, is accompanied by substantial amounts of air entrainment. This manifests as regions of white water in the experiments and low water to air ratio ($w/a < 1$) in the model, and is observed on every step, intensifying as the flow progresses down the steps. The progress to the Transition regime is also predicted well by the numerical model (Fig. 6(b), (e), and (h)) where the longitudinal water surface profile is predicted to change from

Table 2 The statistical calculations of experimental and CFD result Step_2 model with five different discharges

Model	Q m^3/s	Experimental results V_l m/s	CFD model- ling results V_l m/s	The relative error %	RMSE	MAPE %	Correlation (R)
Step_2	0.004	0.147	0.155	5.03	0.021	4.32	0.996
	0.010	0.297	0.312	5.05			
	0.025	0.505	0.492	2.57			
	0.039	0.615	0.638	3.74			
	0.055	0.671	0.706	5.22			

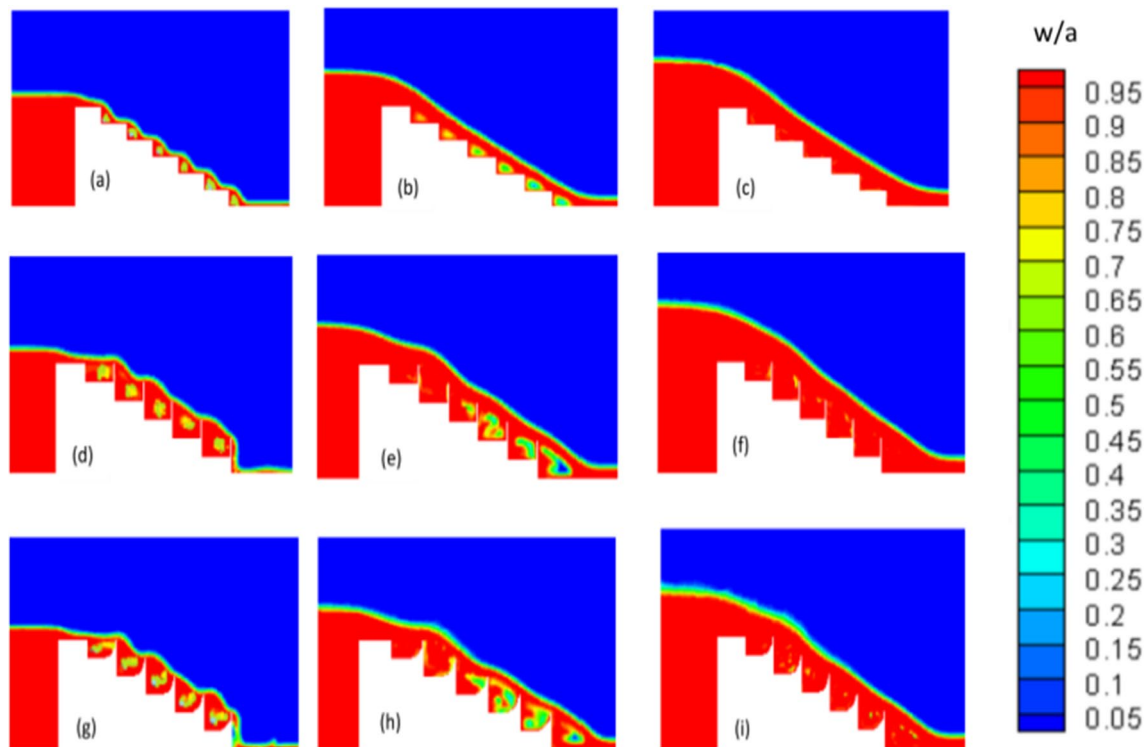


Fig. 6 Modelled free surface and volume fraction of air. Nappe flow: **a** Step_2, **d** Sill_2 and **g** Curve_2, where $q=20.0$ L/s.m, $y_c/h_s=0.69$. Transition flow: **b** Step_2, **e** Sill_2 and **f** Curve_2, where

$20.0 < q < 39.0$ L/s.m, $0.07 \leq y_c/h_s \leq 1.09$. Skimming flow: **c** Step_2 **f** Sill_2 and **i** Curve_2, where $q=39.0$ L/s.m, $y_c/h_s=1.08$

skimming flow (first three steps) to nappe flow (subsequent steps) when $20.0 < q$ (L/s.m) < 39.0 , consistent with the experimental observations. In the experiments (Fig. 4(b), (e) and (h)), it was observed that the flow started out as skimming at the uppermost steps but as the available energy was unable to support skimming flow further downstream, the flow changed to nappe, accompanied by increased air entrainment. These observations are also well supported by the numerical model results in (Fig. 6(b), (e), and (h)). Skimming flow is predicted by the model for larger flow rates ($q \geq 39.0$ L/s.m) where the flow surface appears to be relatively undisturbed, especially for the Step model. For the Sill and Curve geometries, some waviness is seen, due to the obstruction to the flow by the end sills. Model results are shown in Fig. 6(c), (f), and (i), are compared with experimental results shown in Fig. 4(c), (f), and (i), respectively. Except for some slight waviness of the surface, both experimental and numerical water surface profiles are relatively undisturbed, a feature of the skimming flow regime. Air entrainment is also predicted by the model to be less significant, which is confirmed from observations.

An elaboration of the flow patterns is provided by the streamlines plotted in Fig. 6 for Step_2, Sill_2, and Curve_2

models, where differences in step geometry are seen to give rise to differences in the flow direction. In the Curve model, the formation of a strong recirculation region is characterised by a single vortex of regular shape (Fig. 6 (g), (h), and (i)). Significant recirculation is observed for the Curve and Sill models because the end sill deflects the flow around the cavity space, similar to the flow over a cavity. The recirculation flow is more pronounced in the Curve model, generating stronger vortices than in the Sill model. For the Sill model, although the size of the vortex scales with the dimension of the cavity, however, its shape is irregular, and sometimes a secondary, shear-induced vortex (Figs. 6(d), (e), and (f)) is formed at the upstream corner of the sill. For the Step model, a single shear-induced vortex (Fig. 6(a), (b), and (c)), similar to the flow over a backwards-facing step, is produced. The model results provide evidence that links the flow structure with $\Delta E/E_0$ which has been suggested by Felder et al. (2013). It can be postulated that the higher $\Delta E/E_0$ for Curve and Sill models are related to the scale and intensity of vortex structures, which are governed by the step configuration and geometry, and ultimately influences energy dissipation Fig. 7.

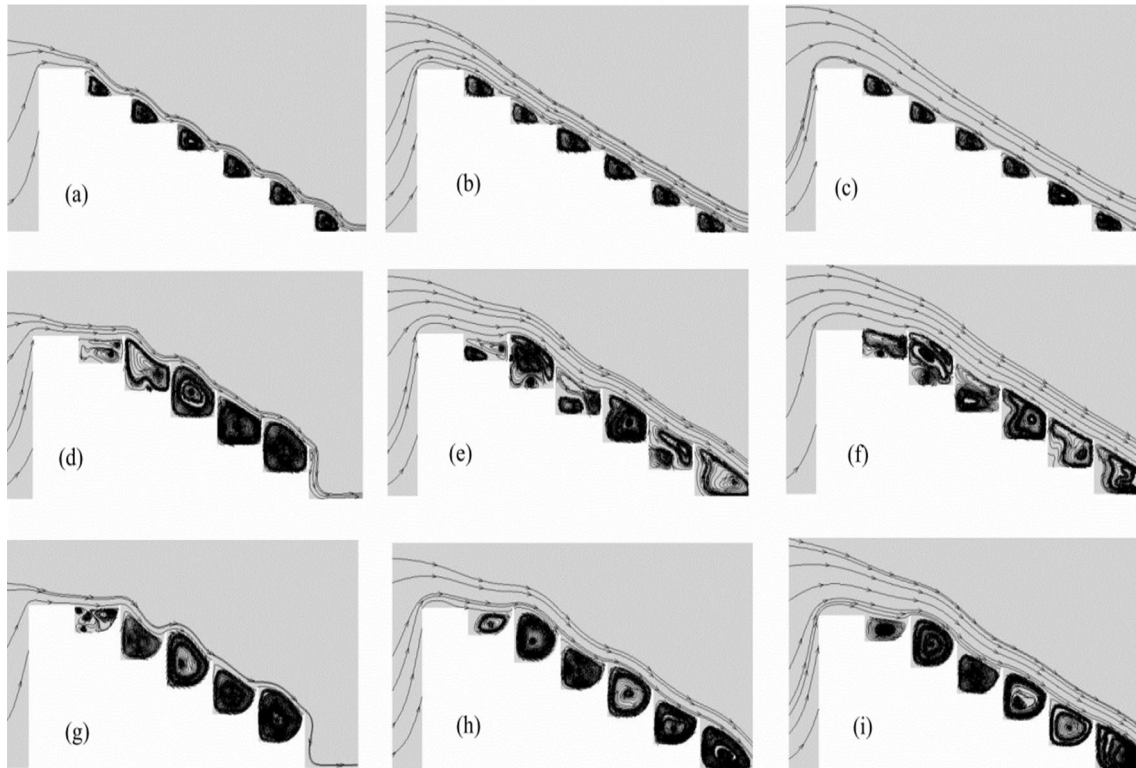


Fig. 7 Flow streamlines. Nappe flow: **a** Step_2, **d** Sill_2 and **g** Curve_2, where $q=20.0$ L/s.m, $y_c/h_s=0.69$. Transition flow: **b** Step_2, **e** Sill_2 and **f** Curve_2, where $20.0 < q < 39.0$ L/s.m,

$0.07 \leq y_c/h_s \leq 1.09$. Skimming flow: **c** Step_2 **f** Sill_2 and **i** Curve_2, where $q=39.0$ L/s.m, $y_c/h_s=1.08$

Stepwise energy dissipation rate

The CFD model results were analysed to study the stepwise energy dissipation. The modelled stepwise energy dissipation rate was investigated using the predicted velocity and flow depth for the downstream edge of each step, to calculate the energy dissipation, incorporating the Bernoulli equation. As before, E_0 is the upstream flow energy and E_i is the energy at the downstream edge for each step, at a distance x from the origin O (Fig. 1) (Zhou et al. 2020):

$$\frac{\Delta E_i}{E_0} = \frac{E_0 - E_i}{E_0} \tag{10}$$

Figure 8 shows the stepwise variation of the nappe, transition, and skimming flow regimes. The x-axis for the models covers a wide range of the discharge (y_c/h_s) showing the $\Delta E_i/E_0$ variations with downstream distance x , or the number of steps when $\theta = 26.6^\circ$. In general, stepwise energy dissipation shows a linear variation with downstream distance and is more distinct between flow regimes when N_s are larger. When $N_s = 10$, it can be observed that $\Delta E_i/E_0$ varies significantly with flow regime according to nappe > transition > skimming. For $N_s = 6$, the number of

steps is presumably too small for the flow regime to be significant. There are significant differences between $\Delta E_i/E_0$ for the Sill and Curve models compared to the Step model. The Step model at any N_s requires a greater distance (or the number of steps) to achieve the same $\Delta E_i/E_0$. Figure 8 also shows that at each step, ΔE_i is high at the nappe flow regime and reduces for transition and skimming flow, which is to be expected. $\Delta E_i/E_0$ is higher for $N_s = 6$ since the step height is larger.

Conclusion

Laboratory experimental work was carried out to investigate energy dissipation rates in stepped spillways. Some results of the laboratory experiments were validated against previous studies. Numerical modelling results were validated against the laboratory data and used to study stepwise energy dissipation behaviour. The conclusions obtained from this study are as follows:

1. Nappe, transition, and skimming flows were observed for all step configurations and geometries investigated.

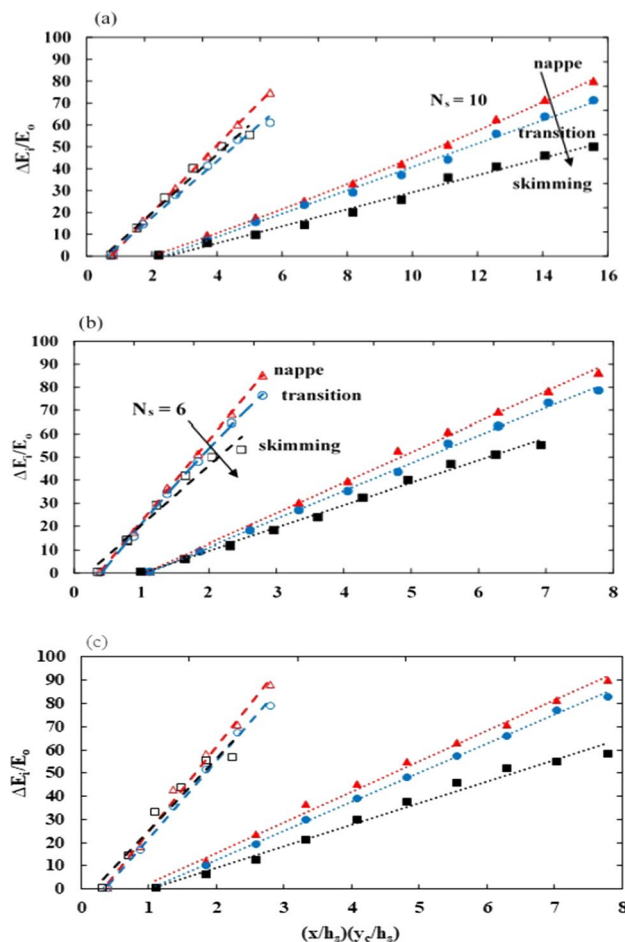


Fig. 8 Energy dissipation over the stepped spillway, **a** Step, **b** Sill and **c** Curve models with $I\theta = 26.6^\circ$

This observation is consistent with past studies conducted on stepped spillways and varied as a function of the step height, step length, step number and discharge. However, the onset of transition and skimming regimes were found to be dependent on step shape, with delay in flow regime change from nappe to transition and to skimming as the discharge was increased.

- Energy dissipation was found to be related to discharge and step shape. The adoption of end sills or curved steps was found to increase energy dissipation rates compared to the traditional steps. In the nappe flow regime, energy dissipation increased by 7% and 5% for the Curve_1 and Sill_1 model respectively, compared to the Step_1 model. The corresponding increase for Curve_2 and Sill_2 models was approximately 10% and 7%, respectively. The increase in energy dissipation reduces with increasing the discharge which means the increase in energy dissipation is less significant in the transition and skimming flow regime.

- Comparisons with numerical predictions showed that the CFD model was able to capture the main flow features when compared to the laboratory experimental results. The water profiles predicted by the CFD model showed good similarity throughout the range of experimental conditions tested. The onset of nappe, transition, and skimming flow regimes predicted by the model for all step shapes corresponded well with the laboratory observations. Investigations of streamlines predicted by the numerical model revealed the influence of step shape on the flow patterns and energy dissipation rates. A strong recirculation with a single vortex of regular shape was predicted for the curve models. For the Sill model, the vortex shape was irregular, occasionally accompanied by a secondary, shear-induced counter-rotating vortex, at the upstream corner of the sill. The Step model is accompanied by a single shear-induced vortex, which was similar to the flow over a backwards-facing step, albeit with a step length much smaller than the re-attachment length.
- The stepwise energy dissipation behaviour showed a linear trend with downstream distance, increasing with the number of steps. The Curve and Sill models had larger energy dissipation than the Step model, for the same distance. This supports the adoption of pooled steps, such as Curve and Sill models as energy dissipation devices. The numerical model reveals that higher energy dissipation rates observed for Curve end Sill models were related to the step heights and lengths which in turn govern the scale and intensity of vortex structures and hence energy dissipation.

Acknowledgements The authors would like to thank all the staff of the Digital Manufacturing and Civil Laboratories at Deakin University for their assistance and support this research.

Author contributions Conceptualization: [UAJ], [RAA], [AC]; Methodology: [UAJ], [AC], [RAA], [AM]; Formal analysis: [UAJ], [RAA], [AC], [AM]; Writing—original draft preparation: [UAJ], [AC], [RAA]; Writing—review and editing: [UAJ], [AC], [RAA], [NAA], [AM], [SAA]; Funding acquisition: [NAA, AM, HSM]; Supervision: [NAA, HSM].

Funding Open access funding provided by Lulea University of Technology.

Declarations

Conflict of interest The authors declare that they have no conflict of interest.

Open Access This article is licensed under a Creative Commons Attribution 4.0 International License, which permits use, sharing, adaptation, distribution and reproduction in any medium or format, as long as you give appropriate credit to the original author(s) and the source, provide a link to the Creative Commons licence, and indicate if changes

were made. The images or other third party material in this article are included in the article's Creative Commons licence, unless indicated otherwise in a credit line to the material. If material is not included in the article's Creative Commons licence and your intended use is not permitted by statutory regulation or exceeds the permitted use, you will need to obtain permission directly from the copyright holder. To view a copy of this licence, visit <http://creativecommons.org/licenses/by/4.0/>.

References

- ANSYS® Academic Research. (2017). Release 18.1, Help System, ANSYS, Inc.
- Castillo, L. G., Carrillo, J. M., García, J. T., & Viguera-Rodríguez, A. (2014). Numerical simulations and laboratory measurements in hydraulic jumps. 11th International Conference on Hydroinformatics, HIC 2014.
- Chanson H (2015) Energy dissipation in hydraulic structures. CRC Press, Boca Raton
- Daneshfaraz R, Ghaderi A, Akhtari A, Di Francesco S (2020) On the effect of block roughness in ogee spillways with flip buckets. *Fluids* 5(4):182. <https://doi.org/10.3390/fluids5040182>
- Dhatrak AI, Tatewar SP (2014) Air entrainment and pressure fields over stepped spillway in skimming flow regime. *J Power Energy Eng* 2(04):53. <https://doi.org/10.4236/jpee.2014.24008>
- Dong Z, Wang J, Vetsch DF, Boes RM, Tan G (2019) Numerical simulation of air–water two-phase flow on stepped spillways behind x-shaped flaring gate piers under very high unit discharge. *Water* 11(10):1956. <https://doi.org/10.3390/w11101956>
- Felder S, Chanson H (2013) Aeration, flow instabilities, and residual energy on pooled stepped spillways of embankment dams. *J Irrig Drain Eng* 139(10):880–887. [https://doi.org/10.1061/\(ASCE\)IR.1943-4774.0000627](https://doi.org/10.1061/(ASCE)IR.1943-4774.0000627)
- Felder S, Chanson H (2015) Aeration and air–water mass transfer on stepped chutes with embankment dam slopes. *Environ Fluid Mech* 15(4):695–710. <https://doi.org/10.1007/s10652-014-9376-x>
- Felder, S. (2013). Air-water flow properties on stepped spillways for embankment dams: Aeration, energy dissipation and turbulence on uniform, non-uniform and pooled stepped chutes. PhD thesis, Queensland University.
- Hamedi A, Ketabdar M (2016) Energy loss estimation and flow simulation in the skimming flow regime of stepped spillways with inclined steps and end sill: a numerical model. *Int J Sci Eng Appl* 5(7):399–407. <https://doi.org/10.7753/IJSEA0507.1006>
- Jahad UA, Al-Ameri R, Das S (2016) Energy dissipation and geometry effects over stepped spillways. *Int J Civ Eng Technol* 7(4):188–198
- Kaouachi A, Carvalho RF, Lopes P, Benmamar S, Gafsi M (2021) Numerical investigation of alternating skimming flow over a stepped spillway. *Water Supply* 21(7):3837–3859. <https://doi.org/10.2166/ws.2021.141>
- Lebdiri F, Seghir A, Berreksi A (2020) Steps number effect on hydraulic parameters of flows in stepped spillways. *Larhyss J* 3(42):41–51
- Lebdiri F, Seghir A, Berreksi A (2022) Multi-objective optimization of stepped spillway and stilling basin dimensions. *Water Supply* 22(1):766–778. <https://doi.org/10.2166/ws.2021.231>
- Li S, Zhang J, Nie J, Peng Y (2014) Energy dissipation and flow characteristics of baffles and sills on stepped spillways. *J Hydraul Res* 52(1):140–142. <https://doi.org/10.1080/00221686.2013.856040>
- Lopez-Egea, M. A. R. T. A., Nistor, I. O. A. N., Townsend, R., Paudel, B. H. U. W. A. N. I., & Sullivan, P. A. U. L. (2015, June). An experimental and numerical study of submerged hydraulic jumps forming at low-head dams. In E-proceedings of the 36th IAHR World Congress (Vol. 28, pp. 24–35).
- Mero S, Mitchell S (2017) Investigation of energy dissipation and flow regime over various forms of stepped spillways. *Water Environ J* 31(1):127–137. <https://doi.org/10.1111/wej.12224>
- Peng SH (2015) Development and application of two-dimensional numerical model on shallow water flows using finite volume method. *J Appl Math Phys* 3(8):989–996. <https://doi.org/10.4236/jamp.2015.38121>
- Roushangar K, Akhgar S, Salmasi F, Shiri J (2014) Modeling energy dissipation over stepped spillways using machine learning approaches. *J Hydrol* 508:254–265. <https://doi.org/10.1016/j.jhydrol.2013.10.053>
- Tabari MMR, Tavakoli S (2016) Effects of stepped spillway geometry on flow pattern and energy dissipation. *Arab J Sci Eng* 41(4):1215–1224. <https://doi.org/10.1007/s13369-015-1874-8>
- Torabi H, Parsaie A, Yonesi H, Mozafari E (2018) Energy dissipation on rough stepped spillways. *Iran J Sci Technol Trans Civ Eng* 42(3):325–330. <https://doi.org/10.1007/s40996-018-0092-5>
- Torrano I, Tutar M, Martinez-Agirre M, Rouquier A, Mordant N, Bourgoïn M (2015) Comparison of experimental and RANS-based numerical studies of the decay of grid-generated turbulence. *J Fluids Eng*. <https://doi.org/10.1115/1.4029726>
- Wu JH, Qian ST, Ma F (2016) A new design of ski-jump-step spillway. *J Hydrodyn* 28(5):914–917. [https://doi.org/10.1016/S1001-6058\(16\)60692-3](https://doi.org/10.1016/S1001-6058(16)60692-3)
- Zhou Y, Wu J, Ma F, Hu J (2020) Uniform flow and energy dissipation of hydraulic-jump-stepped spillways. *Water Supply* 20(4):1546–1553. <https://doi.org/10.2166/ws.2020.056>

Publisher's Note Springer Nature remains neutral with regard to jurisdictional claims in published maps and institutional affiliations.